Electronic Supplementary Information

Synthesis of MoS_2 from $[Mo_3S_7(S_2CNEt_2)_3]I$ for Enhancing Photoelectrochemical Performance and Stability of Cu_2O Photocathode Toward Efficient Solar Water Splitting

Pravin S. Shinde [ab] *Patricia R. Fontenot,* [c] *James P. Donahue,* [c] *Joseph L. Waters,* [bd] *Patrick Kung,* [bd] *Louis E. McNamara,* [e] *Nathan I. Hammer,* [e] *Arunava Gupta,* [abf] *and Shanlin Pan* *, [ab]

[a] Department of Chemistry, [b]Center for Materials for Information Technology, [d]Department of Chemical and Biological Engineering, [f]Department of Electrical and Computer Engineering, The University of Alabama, Tuscaloosa, Alabama 35487, United States

[c] Department of Chemistry, Tulane University, New Orleans, Louisiana 70118, United States

[e] Department of Chemistry and Biochemistry, University of Mississippi, Oxford, Mississippi 38655, United States

* Corresponding Author:

E-mail: span1@ua.edu

Table of Contents

Cyclic voltammetry study of MoS_2 precursors.

Prior to studying redox behaviour of MoS_2 precursors, the ferrocenium/ferrocene (Fc^+/Fc) couple was used as an internal standard for calibration of the electrochemistry set-up. The cyclic voltammogram (Figure S1) of ferrocene in DMF reveals the occurrence of Fc^+/Fc couple at +0.477 V *vs*. Ag/AgCl. The cyclic voltammograms of both $[NH_4]_2[Mo_3S_{13}]$ and $[Mo_3S_7(S_2CNR_2)]^+I^-$ (R = Me or Et) in anhydrous *N*,*N*-dimethylformamide display strong similarity to one another (Figure S2). All of them show an irreversible feature at ~−0.75 V *vs*. Ag/AgCl followed by a reversible reduction at approximately −1.32 V. The dithiocarbamate clusters show an additional irreversible wave upon scanning to ~−1.92 V, which is not apparent in the voltammogram of $[NH_4]_2[Mo_3S_{13}]$. None of the complexes supports any reversible process in the anodic direction. An electrochemical study of $[NH_4]_2[Mo_3S_{13}]$ in CH_2Cl_2 by Garriga, Llusar and coworkers revealed reductions at −1.03 V and −1.27 V ($[Cp_2Fe]^+$/$[Cp_2Fe]$ at + 0.44 V) but no satisfactory explanation about the reversibility of these processes was provided.[1] The irreversibility observed for the first cathodic process may be attributed to transformation of bridging S_2^{2-} ligand to bridging monosulfide, S^{2-}, by extrusion of elemental sulphur from the equatorial positions. This interpretation is suggested by calculations showing the LUMO of $[Mo_3S_{13}]^{2-}$ to be predominantly a σ^* character between sulphur *p* orbitals of the bridging S_2^{2-} ligands.[2] The initial reductions observed for $[Mo_3S_7(S_2CNR_2)]^+I^-$ (R = Me or Et) are notably similar to that in $[Mo_3S_{13}]^{2-}$ both in approximate potentials and qualitative appearance. Thus, the essential basis for irreversibility is likely the same as in $[Mo_3S_{13}]^{2-}$. The reversible following reductions found both in $[Mo_3S_{13}]^{2-}$ and $[Mo_3S_7(S_2CNR_2)]^+I^-$ (R = Me or Et) are tentatively assigned to reduction of the $[Mo_3S_4]^n$ core.

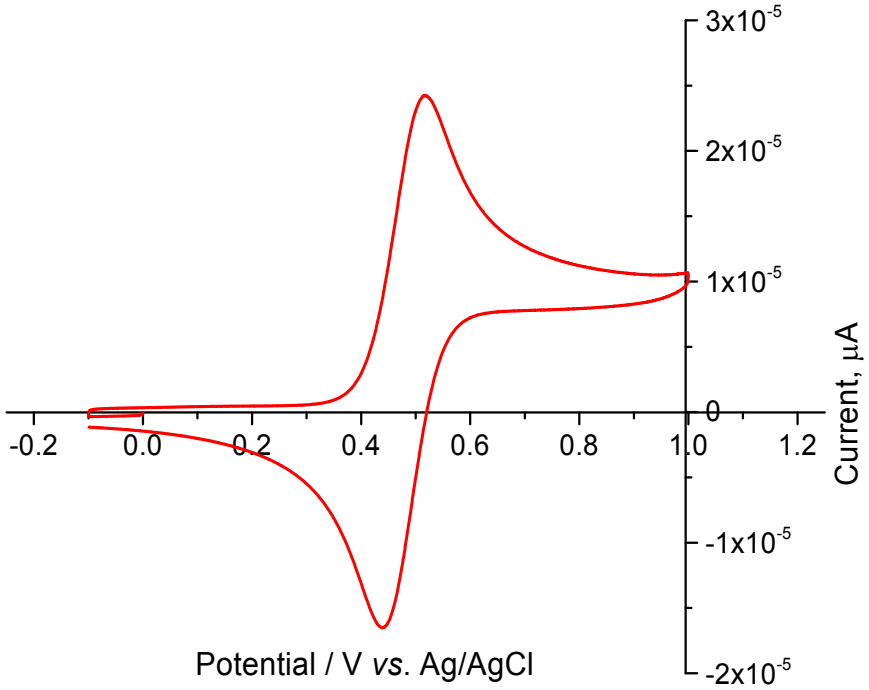

Figure S1. Cyclic voltammogram of ferrocene in DMF showing a ferrocenium/ferrocene couple at +0.477 V *vs*. Ag/AgCl.

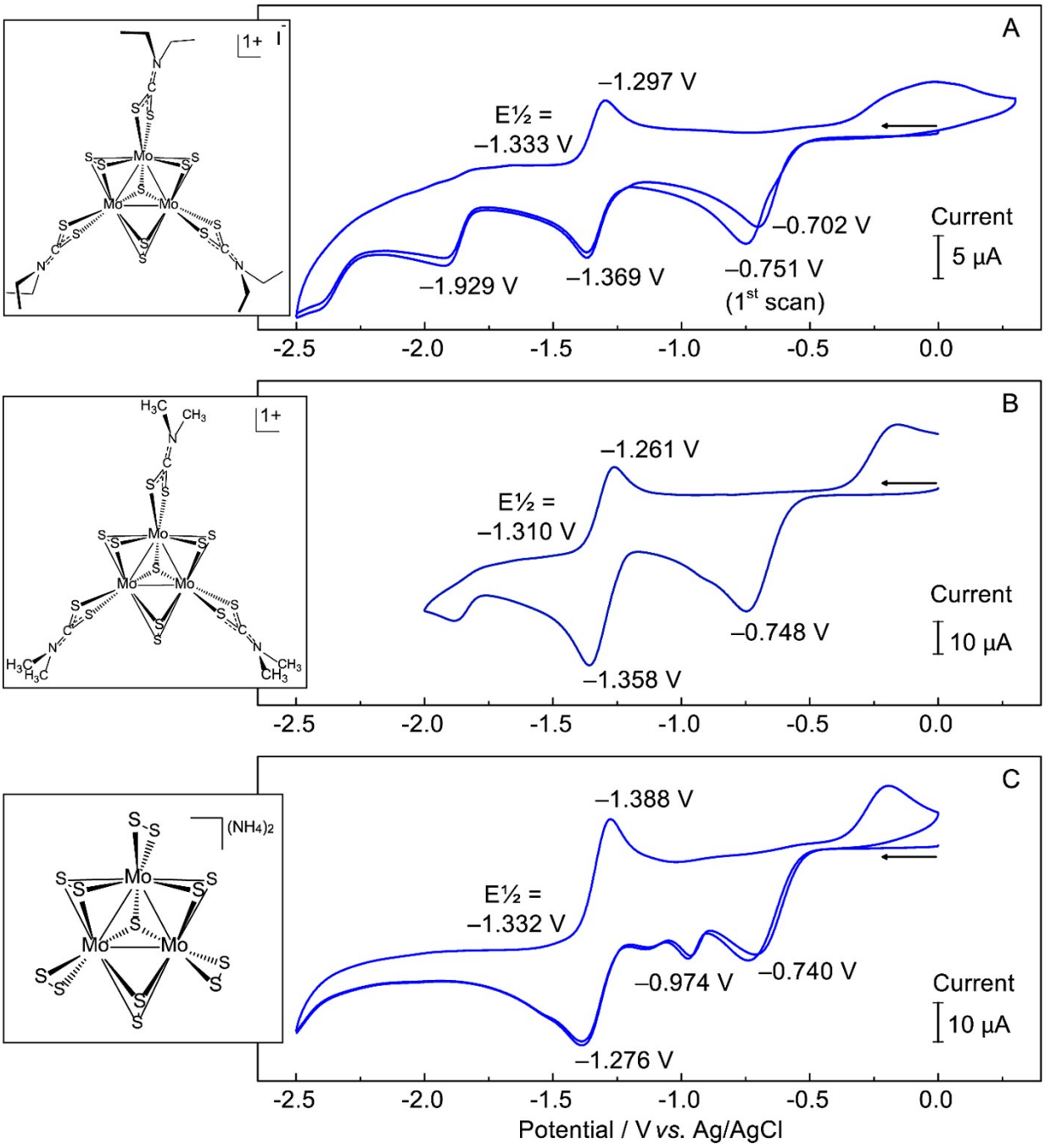

Figure S2. Cyclic voltammograms of (A) $[Mo_3S_7(S_2CNEt_2)_3]I$, (B) $[Mo_3S_7(S_2CNMe_2)_3]I$, and (C) $[NH_4]_2[Mo_3S_{13}]$ in anhydrous DMF. Insets show their corresponding structures.

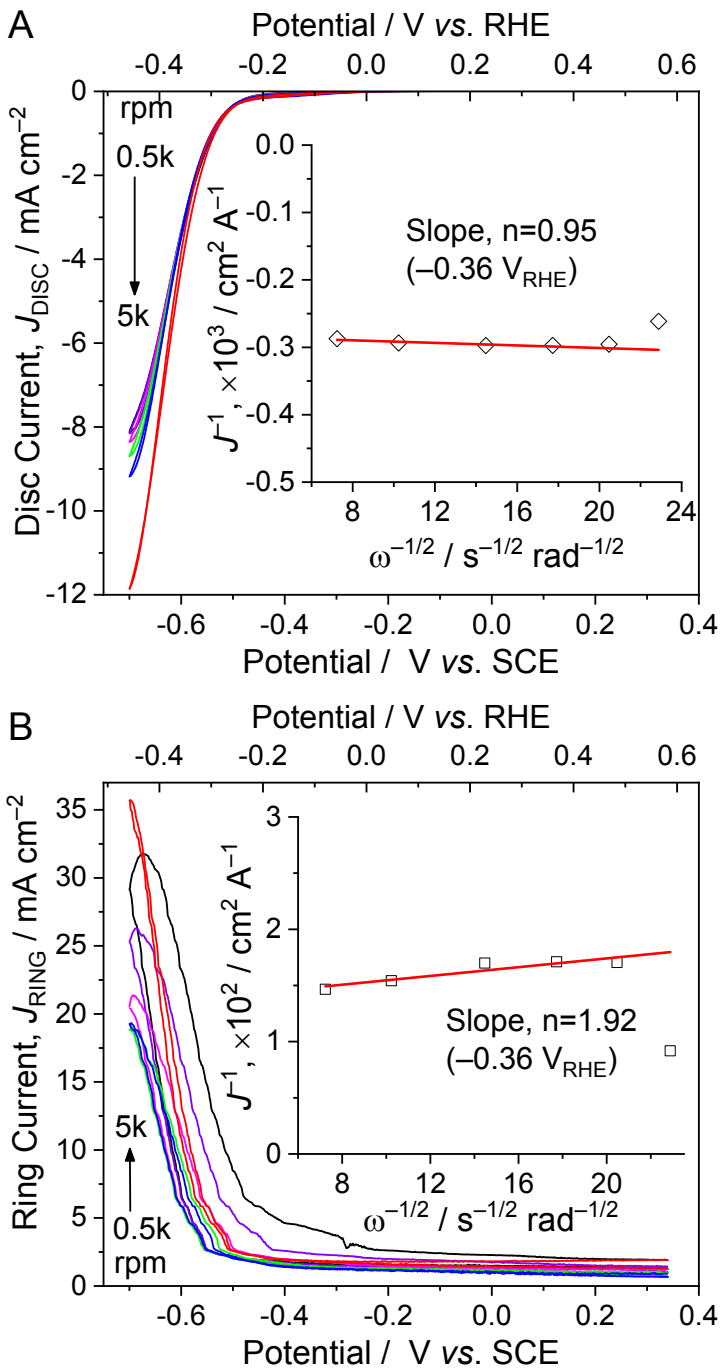

Figure S3. Polarization curves of MoS_2 recorded at (A) disc and (B) ring electrodes at different rotation speeds (viz. 500 to 5000 rpm). Insets show the Koutecky–Levich plots constructed at −0.36 V *vs*. RHE over the entire rotation frequency range at both disc and ring electrodes. Scan rate: 50 mV s^{-1}; Electrolyte: 0.5 M H_2SO_4.

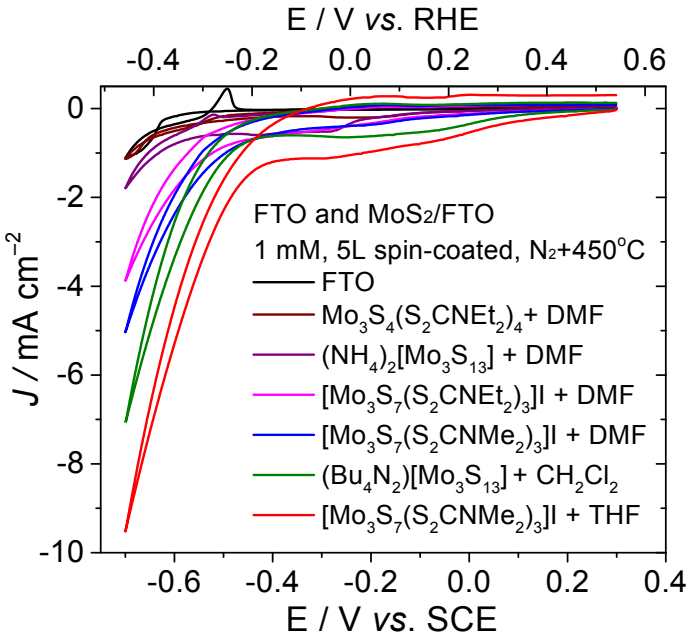

Figure S4. Polarization curves of MoS_2/FTO electrodes fabricated at 450°C in nitrogen environment. Scan rate: 50 mV s^{-1}; Electrolyte: 0.5 M H_2SO_4.

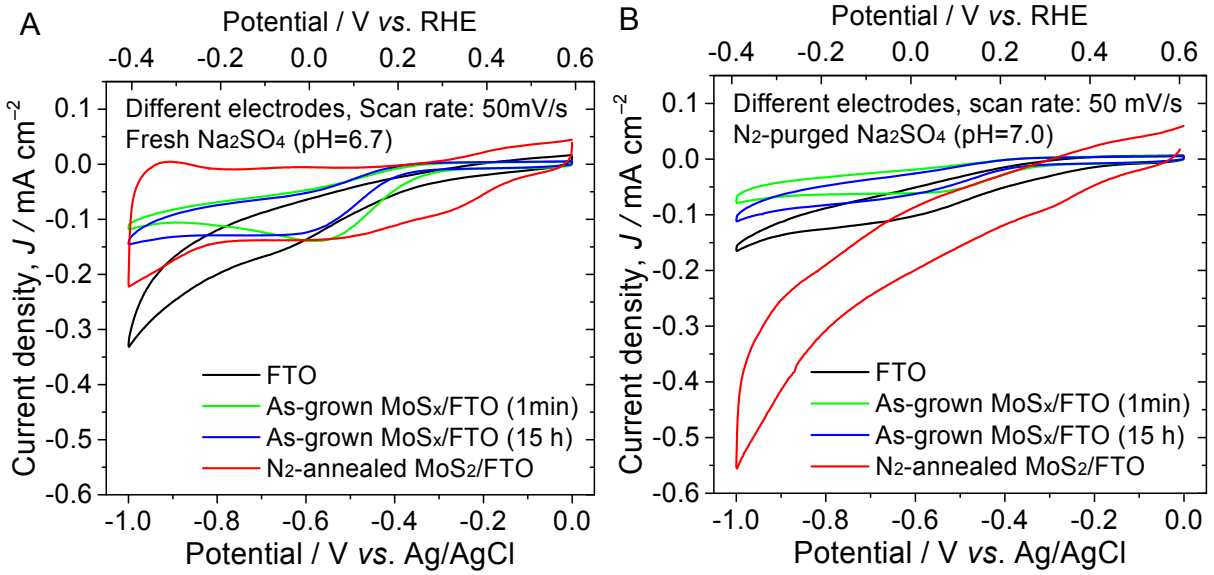

Figure S5. Cyclic voltammograms of bare FTO, as-grown MoS_2 (air-dried for 1 min and 15 h), and N_2-annealed MoS_2 electrodes recorded at the scan rate of 50 mV s^{-1} from (A) freshly prepared and (B) N_2-saturated 0.5 M Na_2SO_4 electrolytes.

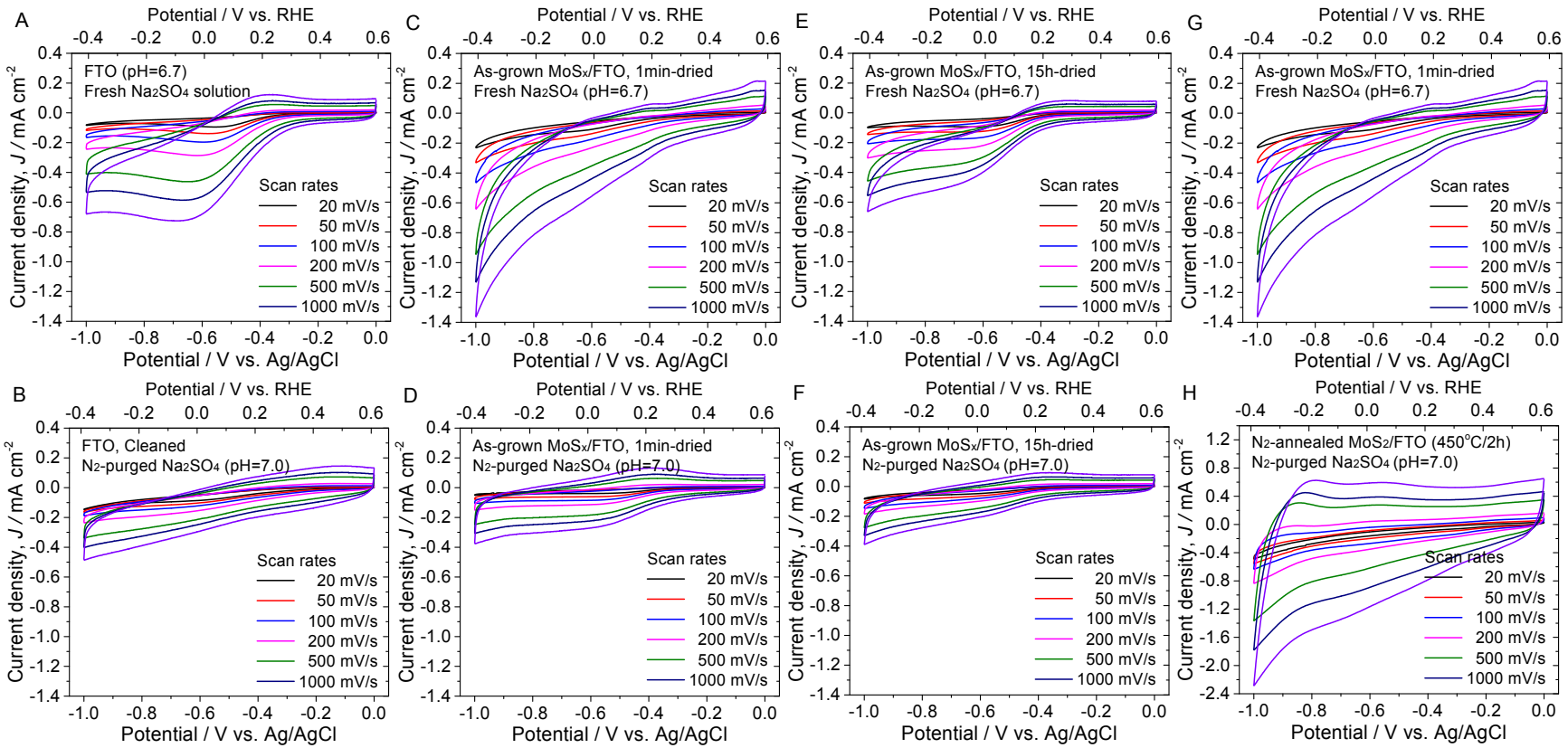

Figure S6. Cyclic voltammograms showing catalytic activity for proton reduction by bare FTO (A, B), as-grown 1-min air-dried MoS_2 (C, D), as-grown 15-h air-dried MoS_2 (E, F), and N_2-annealed MoS_2 (G, H) electrodes from a freshly-prepared and N_2-saturated 0.5 M Na_2SO_4 electrolytes recorded at different scan rates (viz. 20, 50, 100, 200, 500, and 1000 mV s^{-1}).

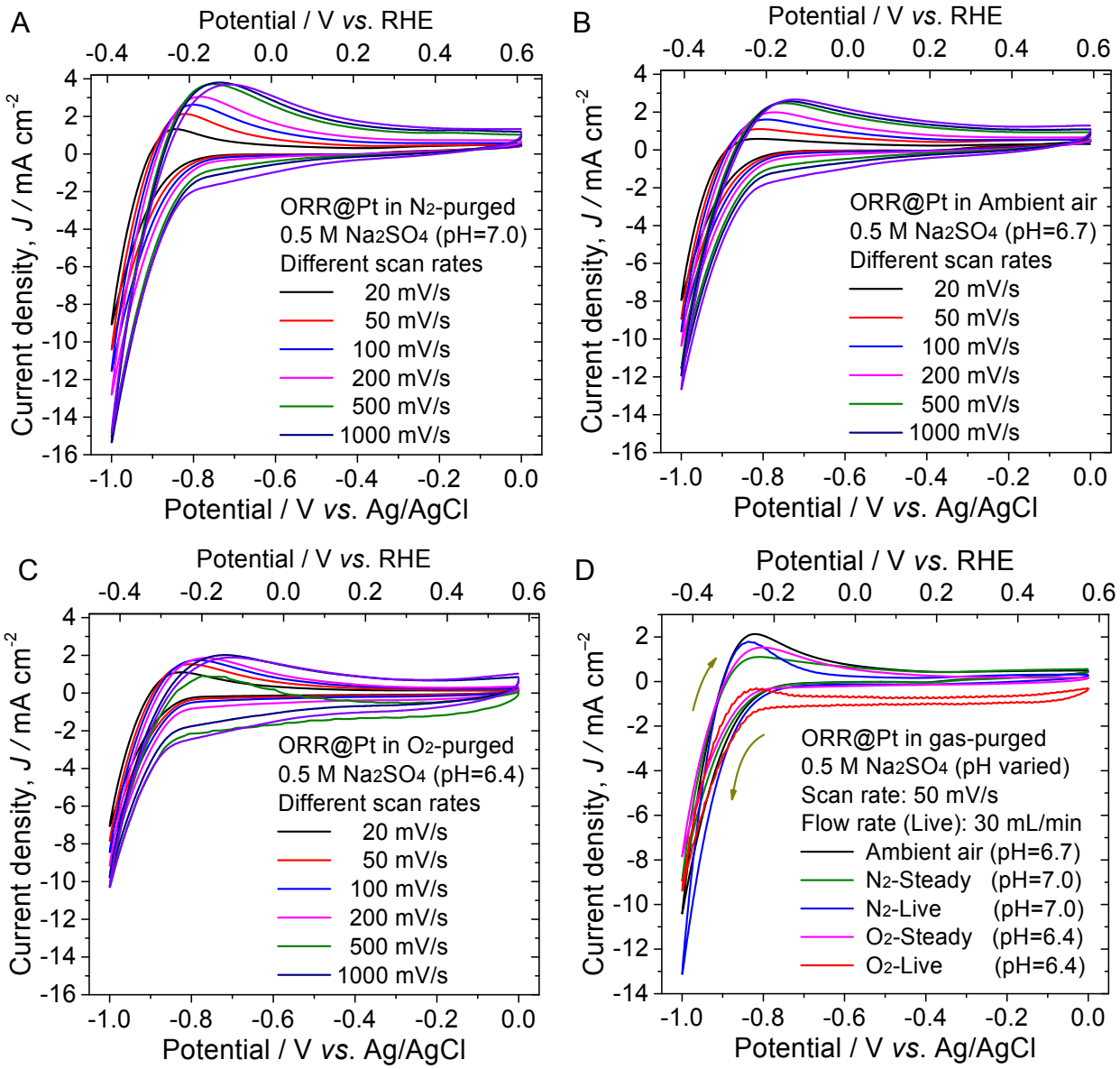

Figure S7. Cyclic voltammograms showing catalytic ORR activity during proton reduction by Pt electrode from (A) 2 h N_2-saturated, (B) freshly-prepared (ambient), and (C) 2 h O_2-saturated 0.5 M Na_2SO_4 electrolytes recorded at different scan rates (viz. 20, 50, 100, 200, 500, and 1000 mV s^{-1}). (D) Overlay of cyclic voltammograms for possible ORR activity at the scan rate of 50 mV s^{-1} for Pt electrode in 0.5 M Na_2SO_4 electrolyte with or without oxygen. CVs were also recorded with in-situ (live) purging of O_2 and N_2 gases at the flow rate of 30 mL cm^{-1}.

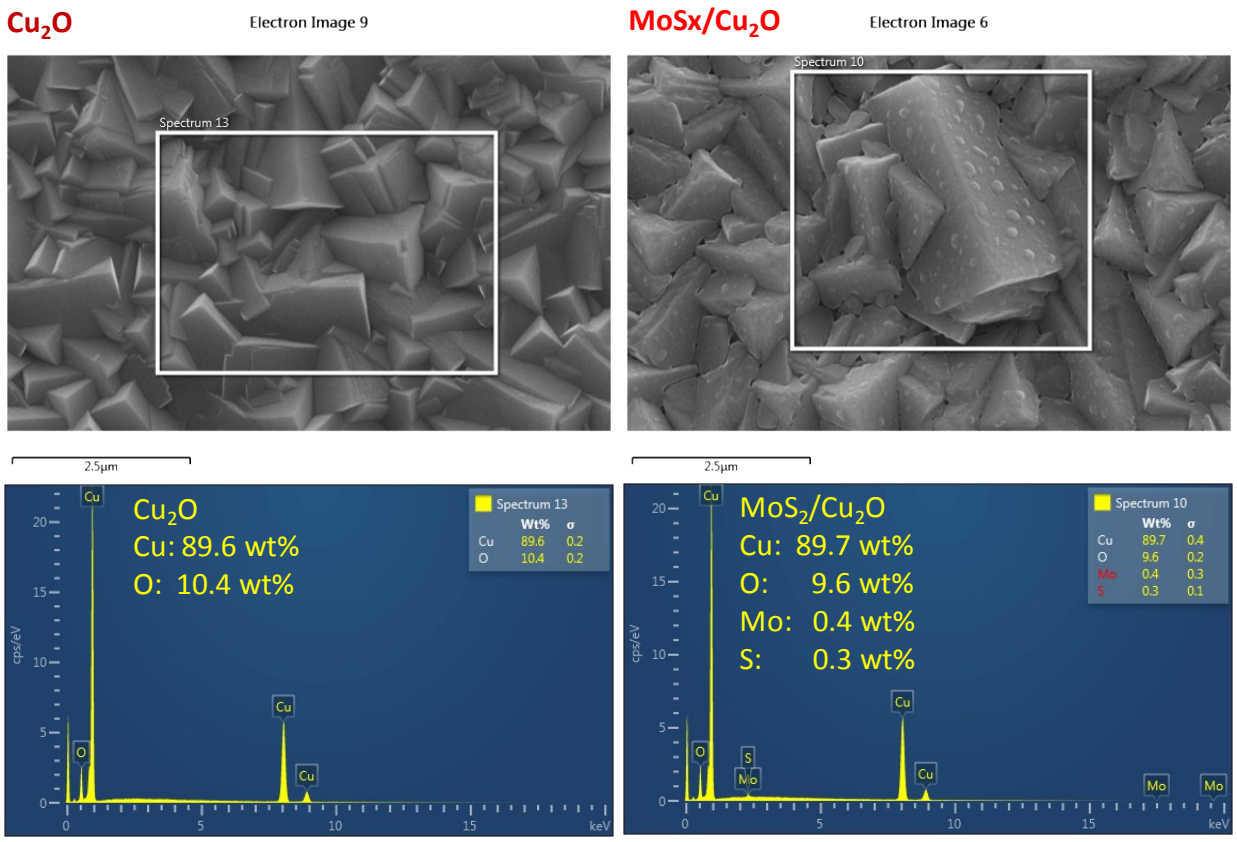

Figure S8. EDS spectra of Cu_2O and MoS_2/Cu_2O samples for elemental confirmation.

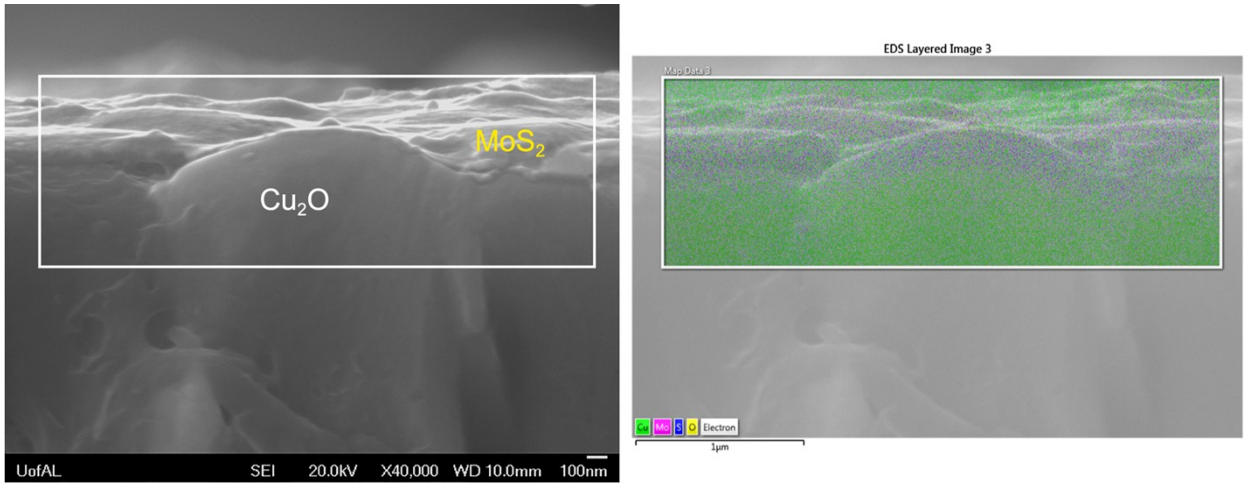

Figure S9. Cross-sectional SEM image (40,000X) of MoS_2-modified Cu_2O revealing coverage of MoS_2 on Cu_2O. A drift in the mapped image is observed due to longer exposure time.

The surface coverage of MoS_2 (n_{MoS_2}) on Cu_2O is estimated using a relation below:[3]

$$n_{MoS_2} = \rho_{MoS_2} * N_A * t_{MoS_2} / MW_{MoS_2}$$

where, ρ_{MoS_2} is the density of MoS_2, N_A is the Avogadro's number, t_{MoS_2} is the film thickness, MW_{MoS_2} is the molar mass of MoS_2.

n_{MoS_2}= (5.06 g cm^{-3} * 6.023 × 10^{23} molecules mol^{-1} * 0.0000040 cm) / (160.07 g mol^{-1})

= 7.6158 × 10^{23}× 10^{-7} molecules cm^{-2}

= 7.6158 ± 0.6 × 10^{16} molecules cm^{-2}

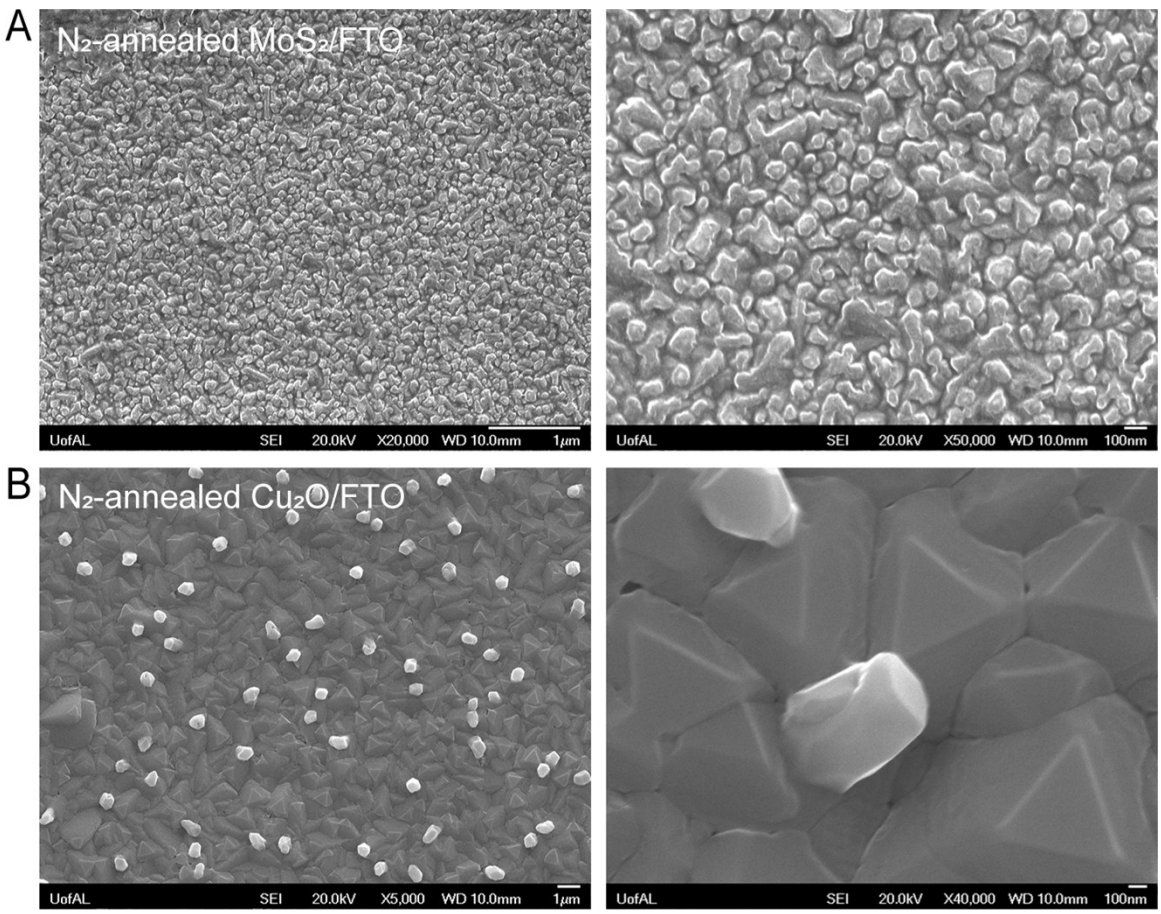

Figure S10. SEM images of (A) N_2-annealed MoS_2 and (B) N_2-annealed Cu_2O on FTO substrate at lower and higher magnifications.

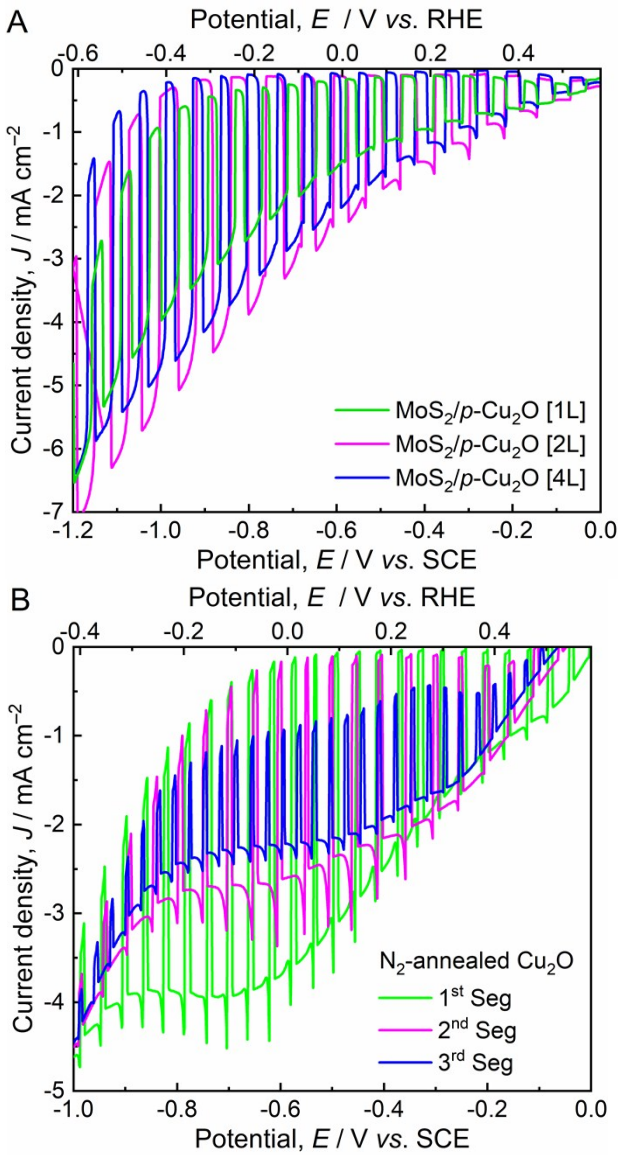

Figure S11. Photocurrent responses of (A) N_2-annealed MoS_2-protected Cu_2O photocathodes (prepared with different spin-coated layers; 1L, 2L, and 4L) and (B) N_2-annealed Cu_2O photocathode (3-segment measurement). Electrolyte: 0.5 M Na_2SO_4 solution (pH ~6.7); Light source: a 300 W Xe lamp; Illumination: simulated 1 sun (100 mW cm^{-2}).

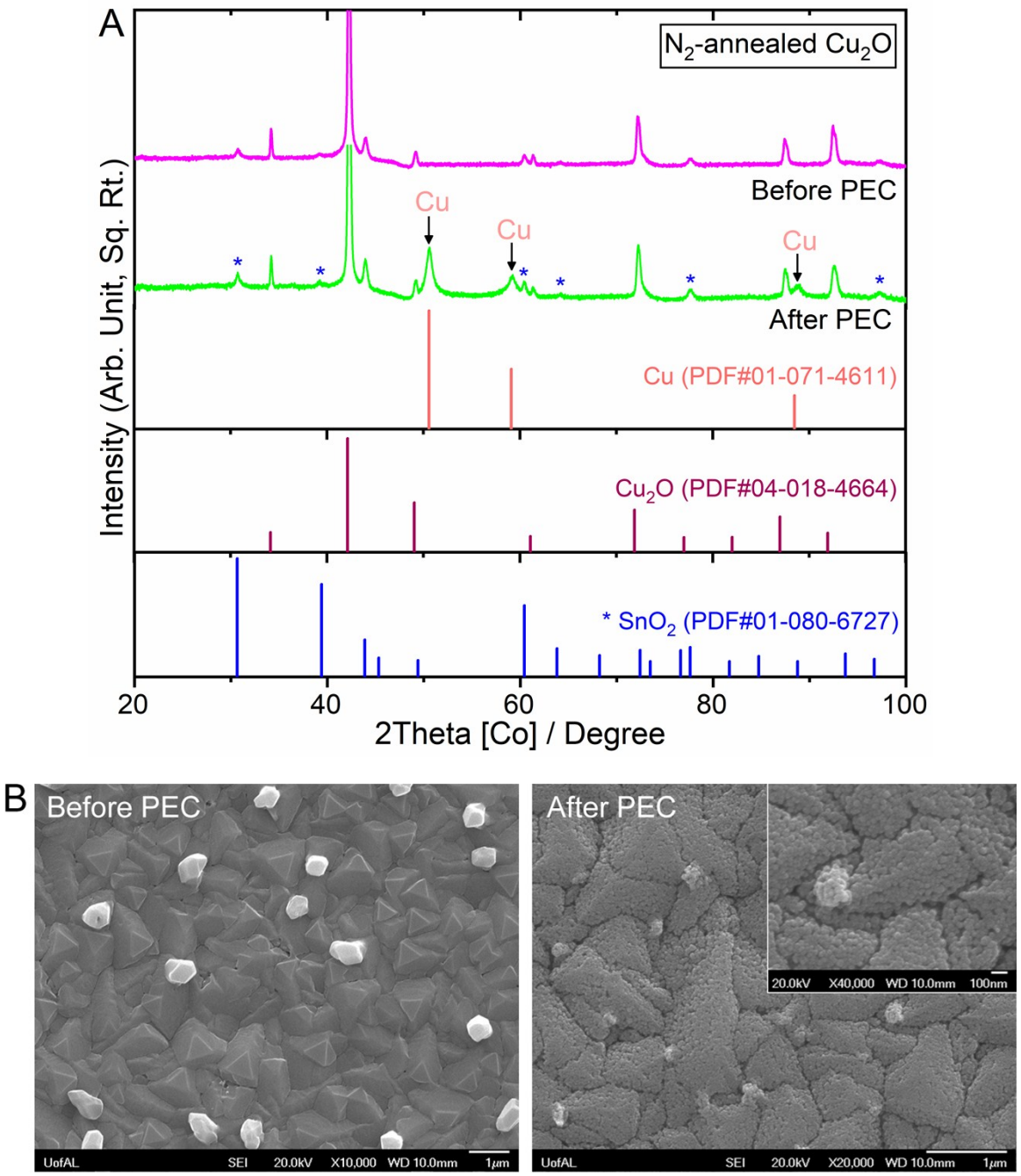

Figure S12. (A) Normalized X-ray diffraction patterns and (B) SEM images (showing porous surface morphology) of N_2-annealed Cu_2O photoelectrode before and after PEC measurement.

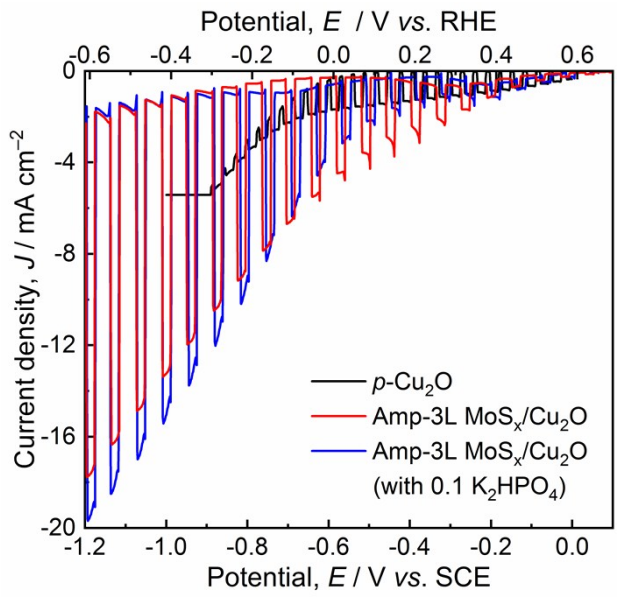

Figure S13. Photocurrent responses of as-grown MoS_x-protected Cu_2O photocathode (with 3L spin-coated MoS_x). Electrolyte: 0.5 M Na_2SO_4 with and without 0.1 M K_2HPO_4 solution; Light source: a 300 W Xe lamp; Illumination: simulated 1 sun (100 mW cm^{-2}).

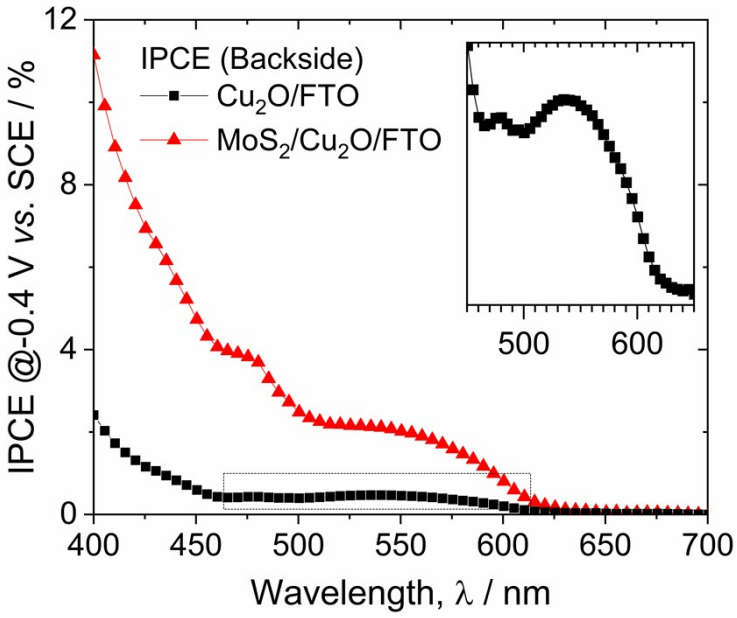

Figure S14. IPCE spectra of as-grown Cu_2O and MoS_2/Cu_2O photocathodes at ~0.2 V *vs*. RHE (−0.4 V *vs*. SCE) under backside illumination. Electrolyte: 0.5 M Na_2SO_4 solution (pH ~6.7).

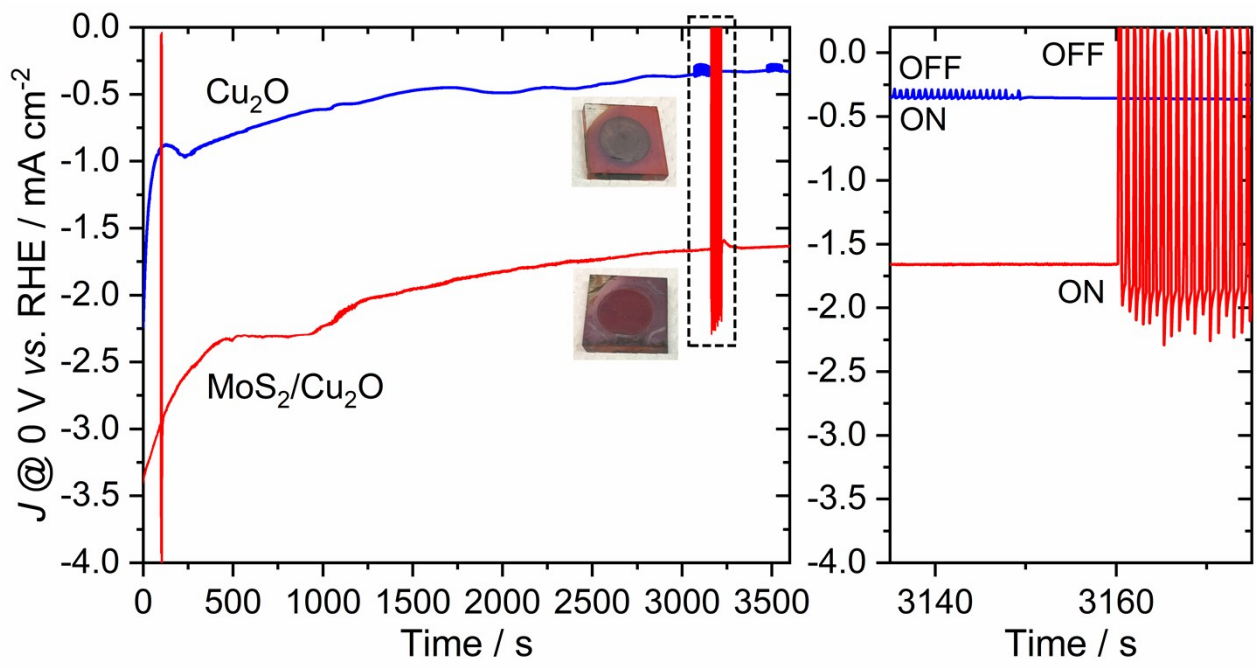

Figure S15. Long-term photostability tests of as-grown Cu_2O and MoS_2-modified Cu_2O photocathodes at an applied potential of 0 V vs. RHE in 0.1 M phosphate buffered (pH ~7) 0.5 M Na_2SO_4 electrolyte.

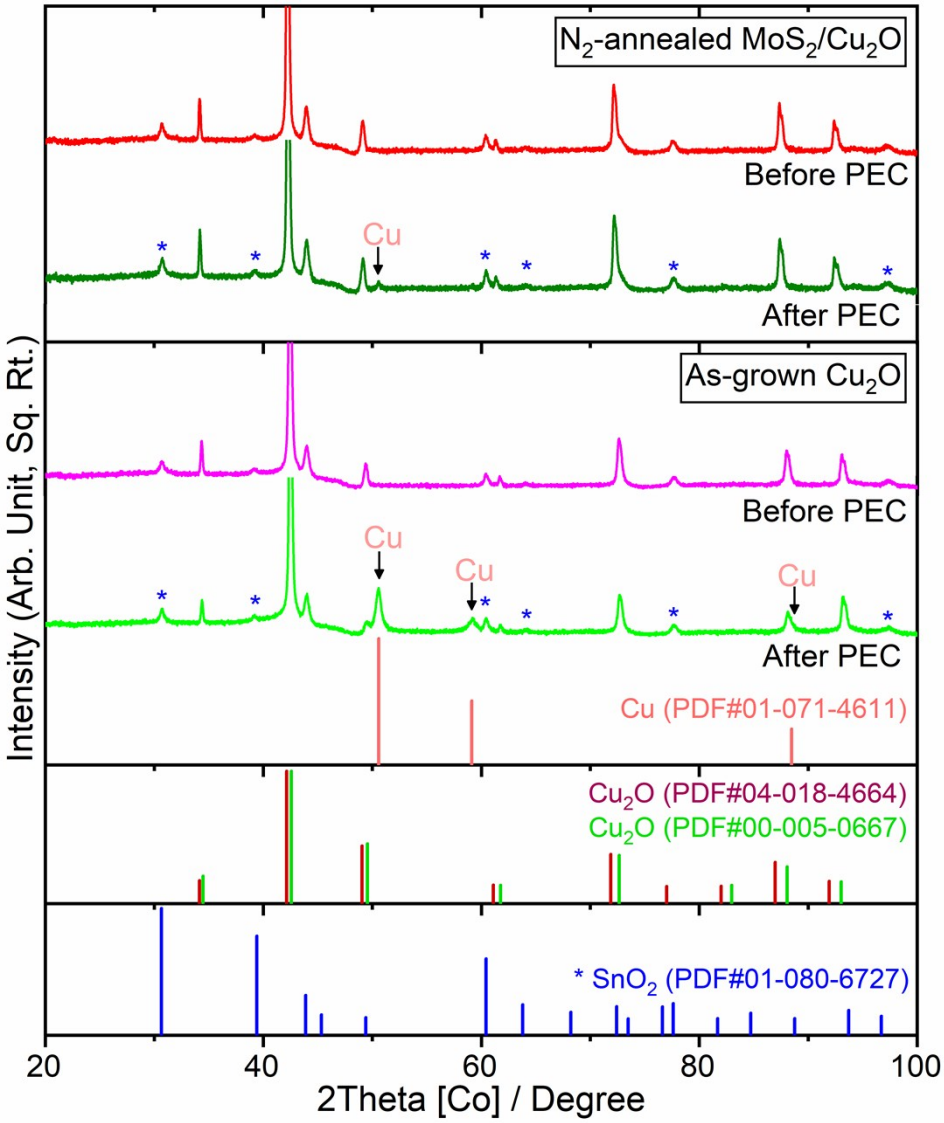

Figure S16. Normalized X-ray diffraction patterns of as-grown Cu_2O and MoS_2-modified Cu_2O photocathodes before and after the 1 h photostability tests.

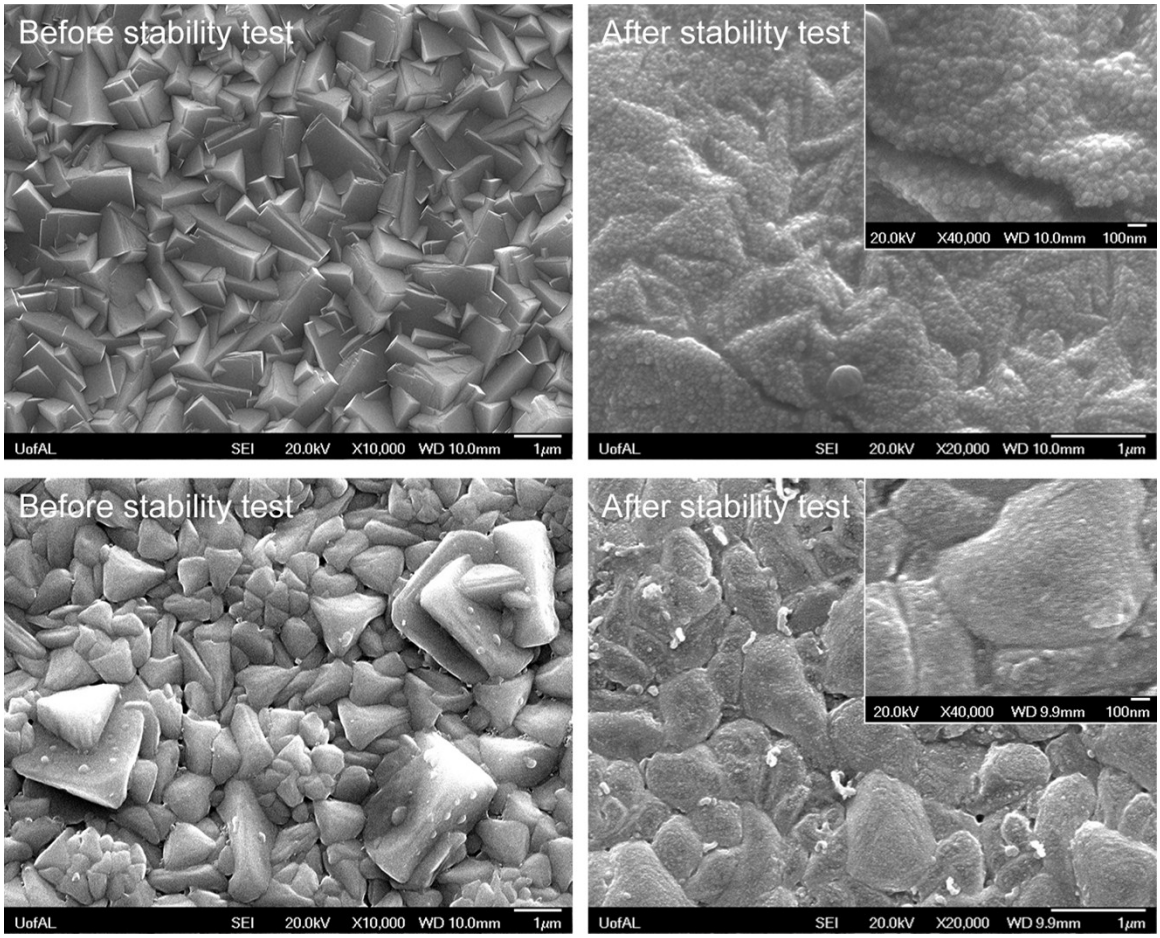

Figure S17. SEM images of (A) as-grown Cu_2O and (B) MoS_2-modified Cu_2O photocathodes before and after the 1 h photostability tests.

References

1. Garriga, J. M.; Llusar, R.; Uriel, S.; Vicent, C.; Usher, A. J.; Lucas, N. T.; Humphrey, M. G.; Samoc, M., *Dalton Trans.* **2003,** 0, 4546-4551.
2. Müller, A.; Wittneben, V.; Krickemeyer, E.; Bögge, H.; Lemke, M., *Z. Anorg. Allg. Chem.* **1991,** 605, 175-188.
3. Ray, S.; Steven, R. T.; Green, F. M.; Höök, F.; Taskinen, B.; Hytönen, V. P.; Shard, A. G., *Langmuir* **2015,** 31, 1921-1930.